ANTICANCER RESEARCH *38*: 5805-5810 (2018)
doi:10.21873/anticanres.12920

Comparative p16^{INK4A} Expression in Laryngeal Carcinoma and Cervical Cancer Precursors: A Real-time Grid-based Immunocytochemistry Analysis

EVANGELOS TSIAMBAS[1,2*], CHRISTOS RIZIOTIS[3*], NICHOLAS S. MASTRONIKOLIS[4], DIMITRIOS PESCHOS[5], ALEXANDROS MORTAKIS[6], GRIGORIOS KYROYSIS[6], STYLIANOS N. MASTRONIKOLIS[7], ANNA BATISTATOU[8], ANDREAS C. LAZARIS[2], EFSTRATIOS PATSOURIS[2] and VASILEIOS RAGOS[9]

[1]*Department of Pathology-Cytology, 401 GA Hospital, Athens, Greece;*
[2]*Department of Pathology, Medical School, University of Ioannina, Ioannina, Greece;*
[3]*Theoretical and Physical Chemistry Institute, National Hellenic Research Foundation, Athens, Greece;*
[4]*ENT Department, Medical School, University of Patras, Patras, Greece;*
[5]*Department of Physiology, Medical School, University of Ioannina, Ioannina, Greece;*
[6]*LITO and IASO-REA, Private Gynaecological Centers, Athens, Greece;*
[7]*Department of Medicine, School of Health Sciences, University of Crete, Heraklion, Greece;*
[8]*Department of Pathology, Medical School, University of Ioannina, Ioannina, Greece*
[9]*Department of Maxillofacial, Medical School, University of Ioannina, Ioannina, Greece*

Abstract. *Background/Aim: p16 (gene locus: 9p21) tumor suppressor gene is considered an important biomarker for the progression and prognosis in a variety of malignancies and pre-cancerous lesions, including high-risk (HR–) human papilloma virus (HPV)-mediated squamous intraepithelial lesions (SILs), based on cytological and the corresponding cervical intraepithelial neoplasia (CIN) histopathological categorization. p16 acts as a cyclin-dependent kinase-4 inhibitor negatively regulating the cell cycle. In persistent HPV infection, E7 oncogenic protein binds retinoblastoma protein leading to its proteolytic transformation, also triggering E2F dissociation, which increases DNA transcription and progression to S phase. This mechanism promotes aberrant p16 over-expression. Our aim was to comparatively analyze p16 protein expression patterns in laryngeal squamous cell carcinomas (LSCC) and also in SILs. Materials and Methods: Fifty (n=50) primary LSCCs tissues all non-HPV-dependent, and a set of 50 liquid-based SILs, were analyzed by immunohistochemistry and immunocytochemistry, respectively. Concerning the screening process in cytological slides, a novel real-time reference and calibration grid platform was implemented and employed. Results: Decreased protein expression was observed in 34/50 (68%) tissues regarding LSCCs. Overall p16 expression was associated to smoking status of the patients (p=0.001), and also with the p-stage of the examined malignancies (p=0.033). A strong statistical significance was assessed correlating LSIL/HSIL cases with a progressive p16 over expression (p=0.001), also reflecting a higher CIN diagnosis (p=0.001). Conclusion: p16 down-regulation is a frequent genetic event in LSCCs, which is associated with advanced disease. In contrast to this, p16 over-expression triggered by a specific molecular mechanism shows a strong relationship with a progressively aggressive phenotype due to upgraded SIL/CIN cervical categorization. The first described application of the grid platform demonstrated a considerable improvement in the immunocytochemistry slide screening process enhancing the diagnostic reliability.*

Cell-cycle deregulation –as a result of imbalanced expression regarding its promoters and inhibitors– critically destabilizes the nuclear micro- environment (1). Among the molecules that regulate cell cycle, p16^{INK4A} abnormal expression plays a crucial role in the progression of pre-cancerous lesions to carcinomas. The gene is located on chromosome 9 (gene

*These Authors contributed equally to this study.

Correspondence to: Evangelos Tsiambas, Cytopathlogist, MD, MSc, PhD, Lecturer elect in Molecular Cytology, Medical School, University of Athens, 17 Patriarchou Grigoriou E΄ Street, Ag. Paraskevi, 153 41 Athens, Greece. Tel: +30 6946939414, e-mail: tsiambasecyto@yahoo.gr

Key Words: p16, laryngeal squamous cell carcinoma, squamous intraepithelial lesion, cervical intraepithelial neoplasia, grid platform, histological categorization.

locus: 9p21) in the cyclin-dependent kinase inhibitor 2A (CDKN2) region, and the corresponding protein acts as a strong inhibitor of cyclin/CDK systems (negative regulator of CDKs 4/6) preventing their phosphorylation (2). Mechanisms of *p16* gene deregulation in malignancies of different histo-genetic types mainly include alterations in its promoter methylation (hypermethylation) and allelic losses (loss of heterozygosity or homozygosity) (3).

Concerning laryngeal squamous cell carcinoma (LSCC), specific missense and frame-shift mutations have been detected leading to decreased $p16^{INK4A}$ expression (4). Interestingly, CDKN2A copy number loss, especially in non-high-risk (HR–) human papilloma virus (HPV)-depended LSCC cases, seems to predict poor survival. Therefore, it could be considered as an independent factor in the corresponding patients (5). Similarly, $p16^{INK4A}$ expression is used as an adjunctive to cytomorphology biomarker for handling female patients diagnosed with HR-HPV-mediated squamous intraepithelial lesions (SILs) based on cytological examination (Papanicolaou test: Pap test). Its aberrant protein over-expression is determined by performing immunocytochemistry (ICC) in liquid-based cytological slides and immunohistochemistry (IHC) in the corresponding cervical intraepithelial neoplasia (CIN) tissue slides (6, 7).

In the current study, the aim was to investigate the $p16^{INK4A}$ protein expression levels in LSCCs and in SILs comparatively. Concerning the ICC slide screening, a novel, recently demonstrated, real-time reference and calibration grid on glass coverslips (Grid Cover Slips; GCS) visualized under conventional bright-field microscope (8, 9) was implemented and employed. To our knowledge this is the first application of this technique in evaluating ICC stained cytological slides, which has also enhanced significantly the reliability of the screening process.

Materials and Methods

Study group. For the purposes of our study, 50 archival, formalin-fixed and paraffin-embedded tissue specimens of histologically confirmed primary LSCCs were used. None of them was HPV-depended (HPV-DNA test negative for all). The hospital ethics committee consented to the use of these tissues in the Department of Pathology, Medical School, University of Ioannina, Greece, for research purposes, according to the World Medical Association Declaration of Helsinki guidelines. The tissue samples were fixed in 10% neutral-buffered formalin. Hematoxylin and eosin (H&E)-stained slides of the corresponding samples were reviewed for confirmation of histopathological diagnoses. All lesions were classified according to the histological typing criteria of the World Health Organization (WHO). Furthermore, a set of 50 liquid-based manually fixed PAP test slides, initially analyzed by implementing an automated system (Cell Solutions CS-30, Menarini, Florence, IT) and stained by PAP method, were used. Slides were provided by the Cytology Unit, Department of Pathology, Medical School, University of Athens, Greece. These cases covered a broad spectrum of abnormal cervicovaginal lesions according to 2014 revised Terminology BETHESDA System (TBS) including low-grade SIL (LGSIL; n=33) and high-grade SIL (HGSIL; n=17) cytological diagnoses. An extra cytological slide of every single case was fixed in order to be immunostained. Concerning the final diagnosis based on biopsy, all tissues were stratified as CIN I: 27, CIN II: 19, and CIN III: 4, respectively.

Antibodies and immunohisto-cytochemistry assay (IHC-ICC). Protein expression levels were determined by the application of ready-to-use monoclonal antibodies: anti-p16INK4 (clone E6H4, Dako Corp., Glostrup, Denmark; dilution at 1:50). IHC for p16 antigen was carried out on 4-μm serial paraffin sections of the corresponding conventional LSCC tissue blocks described above. A slide per case was deparaffinized and rehydrated. En Vision IHC protocol (DAKO Corp.) was performed using an automated IHC staining system (I 6000, Biogenex, Fremont, CA, USA). This IHC protocol is based on a water-soluble dextran polymer system, preventing the endogenous biotin reaction, which is responsible for the background in the stained slides. Briefly, the sections were incubated with the primary antibody for 30 min at room temperature and then incubated with the polymer for 30 min. The antigen-antibody reaction was visualized using 3-3,diaminobenzidine tetrahydrocloride (DAB, Dako Corp.) as a chromogen substrate. Finally, the corresponding sections were slightly counterstained with hematoxylin for 30 sec, dehydrated and mounted. Concerning the cytological samples, the protocol for ICC was similar to IHC, except for omitting the stage of deparaffinization. Protein expression levels were evaluated quantitatively by implementing a digital image analysis protocol (p16 staining intensity levels). For negative control slides, the primary antibody was omitted. According to the manufacturer's guidelines, breast and cervical cancer tissue samples previously reported to strongly express p16 were used as positive control of the staining pattern. A combination of low, moderate, or strong staining intensity, and intracellular, focal, or diffuse nuclear/cytoplasmic localization was acceptable for the specific staining pattern of the marker.

Slide screening process. Screening procedure regarding the p16 immunostained slides was performed under bright field microscopy (microscope Olympus CX-31, Menvile, NY, USA, with ToupView image analysis software, ProWay/ToupTek Protonics, Hangzhou, China) with combined 100×/400× magnification. Concerning the cytological slides, screening was based on a set of coverslips integrated with spatial rectangular grid (GCS) in order to perform a comparative study that would allow the validation of the anticipated enhancement in the screening process using the reference and calibration grid platform, compared to the conventional process.

For the definition of the calibration grid GCS on the coverslips, a novel technique of micromachining was performed, with the use Femtosecond laser in combination with high-precision translation systems for accurately moving the glass coverslips under the laser beams (9). Laser techniques can allow direct writing and transfer of predetermined patterns by means of surface or sub-surface micromachining in a variety of materials ranging from glasses to soft polymeric materials. The technique of femtosecond laser micromachining (FLM) inscription was applied towards the fabrication of a customized visible rectangular grid, on the coverslip of microscope slide (8). The applied FLM inscription set-up is composed by an infrared laser source, generating laser pulses of ~350 fs pulse duration at ~1,064 nm wavelength. The laser beam passes through a power control system in order to adjust its power at the required level, and then it is directed by an optical mirror onto the coverslip flat surface, which is mounted on a three-dimensional XYZ-axis computer-controllable translation stage, for the inscription. The optical delivery

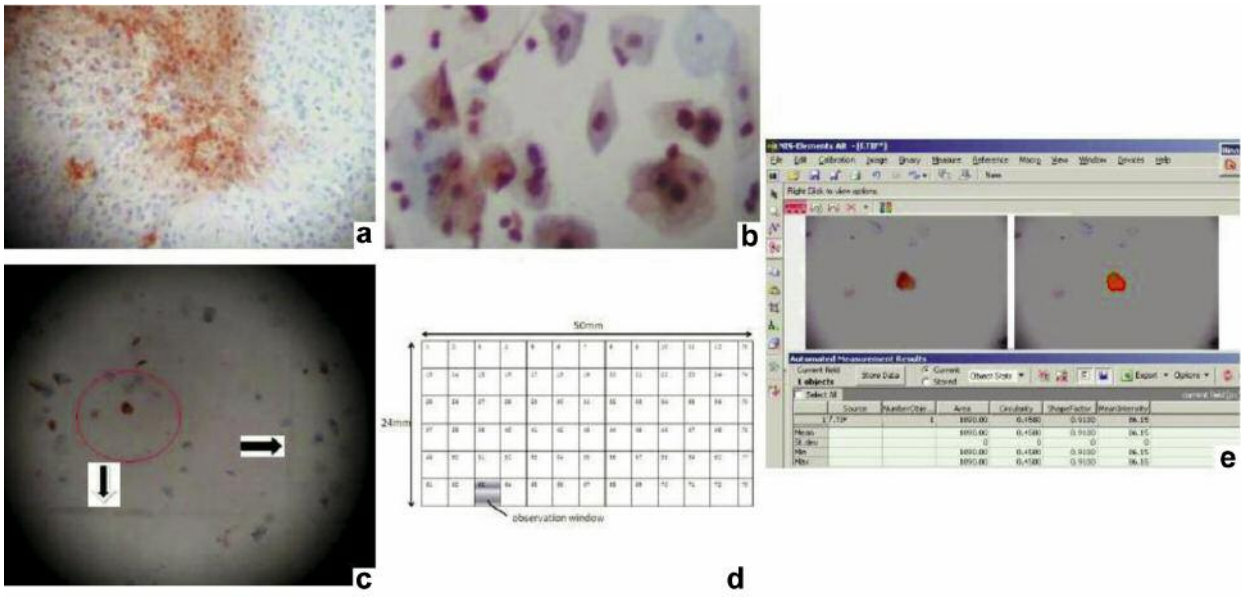

Figure 1. *p16 analysis on tissue and cytological specimens. (a) A tissue section of LSCC with diffuse over-expression of p16. (b) Scattered cells with LSIL cytomorphology with p16 diffuse over-expression. (c) Implementation of a grid-based coverslip on a liquid fixed cytological slide. Arrows show the thin grey lines of the corresponding grid. Inside the red circle, a p16 over-expressing abnormal cell has been detected. (d) Schematic illustration of a spatial grid featuring the segmented and indexed cells as microscopy observation windows. (e) Application of a digital image analysis protocol for estimating p16 protein expression levels. Digitized snapshot of a microscopic field is analyzed by a macro focused on staining intensity values (0-255 at RGB). Red areas show different expression of the marker. The final value is the result of a synthetic approach of all stained pixels (DAB chromogen for p16 ICC&IHC, original magnification 100× and 400×). LSCC, Laryngeal squamous cell carcinoma; LSIL, low-grade squamous intraepithelial lesions; RGB: red green blue; DAB, 3-3,diaminobenzidine tetrahydrocloride; ICC, immunocytochemistry; IHC, immunohistochemistry.*

system of the FLM set-up provides accurate control of laser writing characteristics, such as exposure time, laser beam spot size, laser power density and total delivered laser energy, allowing consequently the accurate control of the laser-based defined grid structures, in terms of geometrical, optical, and surface quality properties (8). That enables the full customization of thickness, and depth, of grid lines in the glass coverslips providing optimum visibility in microscope screening of the corresponding slides, without covering and hiding any vital cytological or biological information. In this study were used commercially available coverslips of length of 50 mm and width of 24 mm and thickness 0.5 mm (Menarini, Florence, Italy) made by typical borosilicate glass. The employed for inscription coverslips in this demonstration example together with the defined grid are schematically illustrated in Figure 1d. This prototype grid consists of 72 rectangular square areas arranged in 12 columns and 6 rows. Each square segment has a typical surface area of 16 mm^2 (4×4 mm). The selected grid pattern size of the employed GCS offered a good balance between the slide segmentation density and the size of the observation window, ensuring an efficient screening of the slide, according to our experience. For the purpose of this study, a set of 50 GCS was constructed. The attachment and employment of these GCS in conventional and liquid-based PAP test specimens have been evaluated and demonstrated through extensive statistical analysis. Based on those results, the reliability and the efficiency of the technique were demonstrated.

Digital image analysis assay (DIA). Expression levels of p16 protein were evaluated quantitatively by calculating the corresponding staining intensity levels. DIA was performed using a semi-automated system (hardware: Microscope CX-31, Olympus, Melville, NY, USA; Digital camera, Sony, Tokyo, Japan; Windows XP/NIS-Elements Software AR v3.0, Nikon Corp., Tokyo, Japan). Areas of interest per tissue section were identified (5 optical fields at 400× magnification) and filed in a digital database. Measurements were performed by implementing a specific macro (diffuse and focal cellular/nuclear protein expression). Based on an algorithm, normal (control) and malignant tissues were measured and the corresponding values of staining intensity levels were compared. A broad spectrum of continuous grey scale values (0-255) at the RedGreenBlue (RGB) analysis was available for discriminating different protein expression levels (Figure 1b). Clinicopathological data of the examined cases and total results are demonstrated in Table I.

Statistical analysis. In order to perform the correlation analysis between the key variables, the statistics software package SPSS v20 (SPSS Inc, Chicago, IL, USA) was used. The first step for this process was to convert all non-numerical variables into numerical values. Associations between protein expression levels and clinicopathological parameters were performed by applying of Pearson Chi-Square (χ^2) test and Spearman's Correlation coefficient. Two-tailed p-values ≤0.05 were considered statistically significant. Results and correlations (p-values) are described in Table I.

Results

According to the protein digital image analysis, all examined cases were evaluated properly demonstrating different p16 expression levels. Decreased (low staining intensity values)

Table I. *Clinicopathological parameters and total p16 expression results.*

Clinicopathological parameters		$p16^{INK4A}$		*p*-Value
LSCC	(n=50)	OE	LE	
	16/50 (32%)	34/50 (68%)		
Gender				0.192
Male	47 (94%)	14/50 (28%)	33/50 (66%)	
Female	3(6%)	2/50 (4%)	1/50 (2%)	
Anatomical region			0. 530	
Supraglotis	14 (28%)	2/50 (4%)	12/50 (24%)	
Glotis	32(64%)	14/50 (28%)	18/50 (36%)	
Subglotis	4 (8%)	0/50 (0%)	4/50 (8%)	
Grade				0.633
1	9 (18%)	2/50 (4%)	7/50 (14%)	
2	29 (58%)	10/50 (20%)	19/50 (38%)	
3	12 (24%)	4/50 (8%)	8/50 (16%)	
Stage				**0.033**
I	4 (8%)	1/50 (2%)	3/50 (6%)	
II	17 (34%)	8/50 (16%)	9/50 (18%)	
III	25 (50%)	5/50 (10%)	20/50 (40%)	
IV	4 (8%)	0/50 (0%)	4/50 (8%)	
Smoking status				**0.001**
Current	42 (84%)	9/50 (18%)	33/50 (66%)	
Former	8 (16%)	6/50 (12%)	2/50 (4%)	
SIL	(n=50)			**0.001**
LSIL	33(66%)	10/50 (20%)	23/50 (46%)	
HSIL	17(34%)	14 /50 (28%)	3/50 (6%)	
CIN				**0.001**
CIN I	27 (54%)	4/50 (8%)	23/50 (46%)	
CIN II	19 (38%)	16/50 (32%)	3/50 (6%)	
CIN III	4 (8%)	4/50 (8%)	0/50 (0%)	

Bold text indicates statistically significant differences. LSCC, Laryngeal squamous cell carcinoma; SIL, squamous intraepithelial lesion; CIN, cervical intraepithelial neoplasia; OE, over-expression (or moderate to high expression, staining intensity values ≤138 at 100% of the examined cells, spectrum between 73 and 138); LE, low expression (staining intensity values >138 at 100% of the examined cells, spectrum between144 and 172).

protein expression was observed in 34/50 (68%) tissues regarding LSCCs. Overall p16 expression was associated to smoking status of the examined patients (p=0.001), and also with the p-stage of the corresponding malignancies (p=0.033). No other statistical correlations were identified concerning the rest clinico-pathological parameters (gender: p=0.192, anatomic location: p=0.530, tumor grade: p=0.633). Concerning the cervicovaginal cytological specimens, a strong statistical significance was assessed correlating LSIL/HSIL cases with a progressive p16 over-expression (p=0.001) also reflecting a higher CIN diagnosis (p=0.001). Furthermore, overall cytological estimation (Pap test diagnosis) was strongly correlated with the CIN categorization provided by biopsy (p=0.001).

Discussion

HR-HPV-depended persistent infection leads to viral DNA integration into the host squamous and metaplastic cell genome in cervicovaginal epithelia. The molecular result of this mechanism is the aberrant transcription of E6/E7 viral oncoproteins leading to SIL development, according to cytomorphological criteria (10). Inside the nuclear microenvironment, HR-HPV E6 protein binds p53 protein inducing its proteolysis. Additionally, HR-HPV E7 protein binds the un-phosphorylated retinoblastoma (Rb) protein providing the same metabolic modification. The direct consequence is the increased release and abnormal transcription of E2F that promotes S phase cell cycle. p16 over-expression is the result of the negative feedback control of the p16 gene transcription by a non-functional Rb protein (11). Concerning LSCCs, the molecular mechanism of p16 over-expression seems to be the same with the cervical SILs described above in the HR-HPV-related cases. In contrast to these, a subset of non-HPV-depended LSCCs have also demonstrated a progressive p16 over expression based on different genetic mechanisms, combined also with the expression of human insulin-like growth factor II mRNA binding protein 3 (IMP3) (12).

In the current study we comparatively analyzed $p16^{INK4A}$ protein expression in SILs and LSCCs implementing ICC and IHC techniques, respectively. Based on our findings by applying DIA protocol for objective measurements regarding the corresponding expression levels, we observed that a significant

proportion of the examined LSCCs demonstrated decreased p16 protein expression, associated with the smoking status of the patients and also with the p-stage of the malignancies. Interestingly, other studies focused on non-HPV-mediated LSCC cases have confirmed that abnormal expression of p16 is related with mutations in its gene locus on chromosome 9p (CDKN2A) (13, 14). Larque *et al*. have detected missense and frame-shift mutations in a series of LSCC patients examined by mRNA and IHC analyses (15). The study group also showed that cases with $p16^{INK4A}$ protein overexpression were progressively correlated to worse survival that was significant for stages I-III. Similarly, another study explored the potential relation between p16 expression and smoking status in LSCC patients. They reported that p16 expression, especially in non-smokers glottic LSCC, should be a promising prognostic factor of better clinical outcome since they demonstrate a low risk of disease recurrence (16). In contrast to the non-HPV related LSCCs, it seems that the role of p16 expression in the HPV-depended is under consideration. Some studies have expressed a serious skepticism regarding the value of the molecule as a reliable surrogate prognostic marker in HPV-infected patients. In one of them, positivity for p16 and/or HPV DNA was not associated with 5-year survival, whereas in another one the prognostic significance of p16 over expression was not assessed because of its infrequency in the examined transcriptionally active HPV-mediated LSCC cases (17).

Concerning SILs, our data showed that the role of p16 overexpression is clear and well-established in comparison to LSCCs. In conjunction with other similar studies, p16 seems to be a reliable prognostic marker for a progressively increased (Low to High) SIL categorization, independently of the HPV DNA HR subtype (18). Additionally, its positive immunoreactivity is used for evaluating borderline or pre-SIL lesions categorized as atypical squamous cells of undetermined significance (ASCUS) (19). Colposcopy combined or not with biopsy, cervicovaginal cell screening provided by Pap test, HPV DNA/mRNA and also p16 ICC/IHC analyses represent a specific protocol for handling the corresponding lesions. Interestingly, significant published data have shown that the combination of tissue morphology and CIN-based categorization with $p16^{INK4a}$ expression analysis is better than morphology alone, increasing also inter-observer agreement in the final cytological estimation (20-24). Morphologic evaluation is a subjective process associated with low interobserver agreement, whereas introduction of IHC/ICC based detection improves interpretation of histopathological and cytological results.

Finally, the current experimental study is characterized by the pilot implementation of an innovative reference and calibration grid on conventional coverslips in the screening process of p16 ICC stained slides. Recently this technique has been successfully performed in cervical screening based on Pap test slides (8). Our study group strongly supports its introduction in routine cytology as a significant improvement in eye-based slide scanning, in detecting abnormal cells that modify diagnoses especially in cytological borderline cases. In this study its diagnostic and research value in screening ICC slides was explored. It was observed that its introduction in this process improved the results. Increased quantity of p16-positive abnormal cells was assessed spotted by slide eye-scanning under conventional bright-field microscopy. Detecting and defining the whole proportion of the abnormal cells and estimating the corresponding protein expression levels by performing DIA protocols is an optimal modern, fast, and accurate approach in gynecological cytology diagnosis and research (25).

Conclusion

Our comparative IHC and ICC study showed that p16 down-regulation is a frequent genetic event in non-HPV-mediated LSCCs, which is associated with advance disease. Concerning HPV-related cervical lesions, p16 over-expression triggered by a specific molecular mechanism (E7 oncogenic activity) shows a strong relationship with a progressively aggressive phenotype due to upgraded SIL/CIN categorization. Novel easy to use applications in real-time slide screening procedures, such as grid-based coverslips, improve diagnosis and research in cytology. Additionally to the aforementioned diagnostic importance of p16 expression, our study showed that this first use of the reference and calibration grid-based method (8, 26) in ICC analysis enhances the diagnostic reliability, providing considerable improvement to the screening process of ICC slides. It is anticipated that further optimization of the method by the use of alternative forms of grid loaded coverslips (26) will improve the screening process.

Conflicts of Interest

The Authors declare no conflicts of interest.

Acknowledgements

This work was supported in part by the project “Advanced Materials and Devices” (MIS 5002409), which is implemented under the “Action for the Strategic Development on the Research and Technological Sector”, funded by the Operational Programme "Competitiveness, Entrepreneurship and Innovation" (NSRF 2014-2020) and co-financed by Greece and the European Union (European Regional Development Fund). The work was also supported by KA 70/3/723 research program Medical School, University of Athens, Greece. COST Action BM1401 "Raman based applications for clinical diagnostics- Raman4Clinics", and COST Action MP1401: "Advanced fibre laser and coherent source as tools for society, manufacturing and lifescience" are also acknowledged. Authors acknowledge the significant scientific contribution of George Vilaras, Technologist in Dept of Pathology, Medical School, University of Athens, Athens, Greece as an expert in IHC/ICC techniques and also Eleftherios Stavrakas, MEng, MSc, PMI-RMP, CEng, PRINCE2 Consultant, Germany, for his extensive statistical analysis.will improve the screening process.

References

1 Hanahan D and Weinberg RA: Hallmarks of cancer: The Next Generation. Cell *144*: 646-674, 2011.

2 Huang K, Li LA, Meng YG and Fu XY : p16 expression in patients with cervical cancer and its prognostic significance: meta-analysis of published literature. Eur J Obstet Gynecol Reprod Biol *183*: 64-69, 2013.

3 Kim J, Kim MA, Min SY, Jee CD, Lee HE and Kim WH: Downregulation of methylthioadenosin phosphorylase by homozygous deletion in gastric carcinoma. Genes Chromosomes Cancer *50(6)*: 421-433, 2011.

4 Strzelczyk JK, Krakowczyk Ł and Owczarek AJ: Aberrant DNA methylation of the p16, APC, MGMT, TIMP3 and CDH1 gene promoters in tumours and the surgical margins of patients with oral cavity cancer. J Cancer *9(11)*: 1896-1904, 2018.

5 Chen WS, Bindra RS, Mo A, Hayman T, Husain Z, Contessa JN, Gaffney SG, Townsend JP and Yu JB: CDKN2A copy number loss is an independent prognostic factor in HPV-negative head and neck squamous cell carcinoma. Front Oncol *4(8)*: 95-100, 2018.

6 Gustinucci D, Giorgi Rossi P and Cesarini E: Use of cytology, E6/E7 mRNA, and p16INK4a-Ki-67 to define the management of human papillomavirus (HPV)-positive women in cervical cancer screening. Am J Clin Pathol *145(1)*: 35-45, 2016.

7 Bergeron C, Ronco G, Reuschenbach M, Wentzensen N, Arbyn M, Stoler M and von Knebel Doeberitz M: The clinical impact of using p16(INK4a) immunochemistry in cervical histopathology and cytology: an update of recent developments. Int J Cancer *136(12)*: 2741-2751, 2015.

8 Tsiambas E and Riziotis C: Implementation of a Real-Time Reference and Calibration Grid Platform for Improved Screening - Mapping in Pap test Slides. Pathol Int *67*: 24-31, 2017.

9 Riziotis C and Tsiambas E: Grid-based visual aid for enhanced microscopy screening in diagnostic cytopathology. Proc. SPIE 10024, Optics in Health Care and Biomedical Optics VII, 100244M, 2016.

10 Kalli K, Riziotis C, Posporis A, Markos C, Koutsides C, Ambran S, Webb AS, Holmes C, Gates JC, Sahu JK and Smith PGR: Flat fibre and femtosecond laser technology as a novel photonic integration platform for optofluidic based biosensing devices and lab-on-chip applications: current results and future perspectives. Sensors and Actuators B. Chemical *209*: 1030-1040, 2015.

11 Ukpo OC, Flanagan JJ, Ma XJ, Luo Y, Thorstad WL and Lewis JS Jr.: High-risk human papillomavirus E6/E7 mRNA detection by a novel in situ hybridization assay strongly correlates with p16 expression and patient outcomes in oropharyngeal squamous cell carcinoma. Am J Surg Pathol *35(9)*: 1343-1350, 2011.

12 Wentzensen N and von Knebel Doeberitz M: Biomarkers in cervical cancer screening. Dis Markers *23*: 315-330, 2007.

13 Orsaria M, Marzinotto S, De Marchi L, Giacomarra V, Boria S, Rubini C, Londero AP, Di Loreto C and Mariuzzi L: HPV-related Oropharyngeal Squamous Cell Carcinoma: $p16^{INK4A}$ Immunohistochemistry or HPV Genotyping? Anticancer Res *35(9)*: 4733-4739, 2015.

14 Riener MO, Hoegel J, Iro H, Hartmann A and Agaimy A: IMP3 and p16 expression in squamous cell carcinoma of the head and neck: A comparative immunohistochemical analysis. Oncol Lett *14(2)*: 1665-1670, 2017.

15 Larque AB, Conde L, Hakim S, Alos L, Jares P, Vilaseca I, Cardesa A and Nadal A: P16(INK4a) overexpression is associated with CDKN2A mutation and worse prognosis in HPV-negative laryngeal squamous cell carcinomas. Virchows Arch *466(4)*: 375-382, 2015.

16 Kalfert D, Celakovsky P, Laco J and Ludvikova M: The role of protein p16(INK4a) in glottic laryngeal squamous cell carcinoma. Pathol Oncol Res *20(4)*: 909-915, 2014.

17 Ciesielska U, Zatonski T, Nowinska K, Ratajczak-Wielgomas K, Grzegrzolka J, Piotrowska A, Olbromski M, Pula B, Podhorska-Okolow M and Dziegiel P: Expression of cell cycle-related proteins p16, p27 and Ki-67 proliferating marker in laryngeal squamous cell carcinomas and in laryngeal papillomas. Anticancer Res *37(5)*: 2407-2415, 2017

18 Hernandez BY, Rahman M, Lynch CF, Cozen W, Unger ER, Steinau M, Thompson T, Saber MS, Altekruse SF, Goodman MT, Powers A, Lyu C and Saraiya M: p16(INK4A) expression in invasive laryngeal cancer. Papillomavirus Res 2: 52-55, 2016.

19 Young RJ, Urban D, Angel C, Corry J, Lyons B, Vallance N, Kleid S, Iseli TA, Solomon B and Rischin D: Frequency and prognostic significance of p16(INK4A) protein overexpression and transcriptionally active human papillomavirus infection in laryngeal squamous cell carcinoma. Br J Cancer *112(6)*: 1098-104, 2015.

20 Kisser A and Zechmeister-Koss I: A systematic review of p16/Ki-67 immuno-testing for triage of low grade cervical cytology. BJOG *122(1)*: 64-70, 2015.

21 Huang K, Li LA, Meng YG and Fu XY: p16 expression in patients with cervical cancer and its prognostic significance: meta-analysis of published literature. Eur J Obstet Gynecol Reprod Biol *183*: 64-69, 2014.

22 Gurrola-Díaz CM, Suárez-Rincón AE, Vázquez-Camacho G, Buonocunto-Vázquez G, Rosales-Quintana S, Wentzensen N, von Knebel Doeberitz M: P16INK4a immunohistochemistry improves the reproducibility of the histological diagnosis of cervical intraepithelial neoplasia in cone biopsies. Gynecol Oncol *111(1)*: 120-124, 2008.

23 Bergeron C, Ordi J, Schmidt D, Trunk MJ, Keller T and Ridder R; European CINtec histology study group: Conjunctive $p16^{INK4a}$ testing significantly increases accuracy in diagnosing high-grade cervical intraepithelial neoplasia. Am J Clin Pathol *133(3)*: 395-406, 2010.

24 Reuschenbach M, Wentzensen N, Dijkstra MG, von Knebel Doeberitz M and Arbyn M: $p16^{INK4a}$ immunohistochemistry in cervical biopsy specimens: A systematic review and meta-analysis of the interobserver agreement. Am J Clin Pathol *142(6)*: 767-772, 2014.

25 Tsiambas E, Riziotis C, Mavrikos I, Armatas E and Patsouris E: Novel techniques for morphometric and geometrical analysis in squamous intraepithelial lesions on cervical smears. JBUON *22(4)*: 1081-1083, 2017.

26 Riziotis C and Tsiambas E: Reference and Calibration Grid for Medical Diagnostic Microscopy, Patent Application, WO2017/009673, PCT/GR2016/000032, GR Patent #1008931, 2017.

Received August 31, 2018
Revised September 22, 2018
Accepted September 24, 2018